

## Formation of InPAs solid solutions by solid phase substitution method

© G.S. Gagis, V.I. Kuchinskii, D.Yu. Kazantsev, B.Ya. Ber, M.V. Tokarev, V.I. Vasilev

Ioffe Institute, St. Petersburg, Russia  
E-mail: gsgagis@mail.ioffe.ru

Received November 1, 2025  
Revised November 25, 2025  
Accepted November 29, 2025

The samples obtained by the method of solid phase substitution of the fifth group elements in InP with arsenic and in InAs with phosphorus during  $\tau = 30$  and 70 min at temperatures  $t = 585$  and  $655$  °C are investigated. According to secondary ion mass spectrometry data, the elements of the fifth group penetrated to a depth of 100 nm. For InP, the amount and depth of penetration of arsenic at the same  $\tau$  and  $t$  differed with different types of doping of the substrates.

**Keywords:** Solid-phase substitution, indium arsenide, indium phosphide, zinc diffusion, secondary ion mass spectrometry.

DOI: 10.61011/TPL.2026.03.63074.20554

The method of fabricating a  $p-n$ -junction by diffusing an acceptor Zn impurity from the vapor phase into an  $n-A^{III}B^V$  wafer [1] remains relevant to the production of optoelectronic devices, such as photovoltaic converters based on GaAs and GaSb. We have already demonstrated that a similar method may be used for solid-phase substitution of fifth-group elements  $B^V$  in an  $A^{III}B^V$  wafer with different fifth-group elements  $C^V$ , which promotes the formation of a near-surface layer of a solid solution and obtaining an  $A^{III}B_{1-x}^V C_x^V/A^{III}B^V$  heterostructure [2]. Alongside with solid-phase substitution, one may perform diffusion of a  $D^{II}$  (Zn or Cd) impurity; an  $A^{III}B^V$   $n$ -type wafer should then be used to form the  $p-n$ -junction. The possible sources of dopant  $D^{II}$  impurities and fifth-group elements  $C^V$  are solution-melts that include these components. It is convenient to use solution-melts of the  $Sn-D^{II}E^{IV}C_2^V$  type.

The main factors influencing the distribution of substitution components  $C^V$  and the diffusing dopant impurity in the initial  $A^{III}B^V$  wafer are process temperature  $t$ , holding time  $\tau$ , and substitution component vapor pressure  $P_C$ , which depends to a significant extent on  $t$  and atomic fraction  $x_C^L$  of component  $C^V$  in the solution-melt. The qualitative and quantitative composition of the solution-melt and the chemical nature of the initial  $A^{III}B^V$  wafer and substitution element  $C^V$  are also important, which was discussed in more detail in [2]. In general, the processes accompanying solid-phase substitution depend on a fairly large number of different factors and cannot be characterized theoretically with sufficient accuracy; therefore, experimental studies are needed for successful fabrication of device structures.

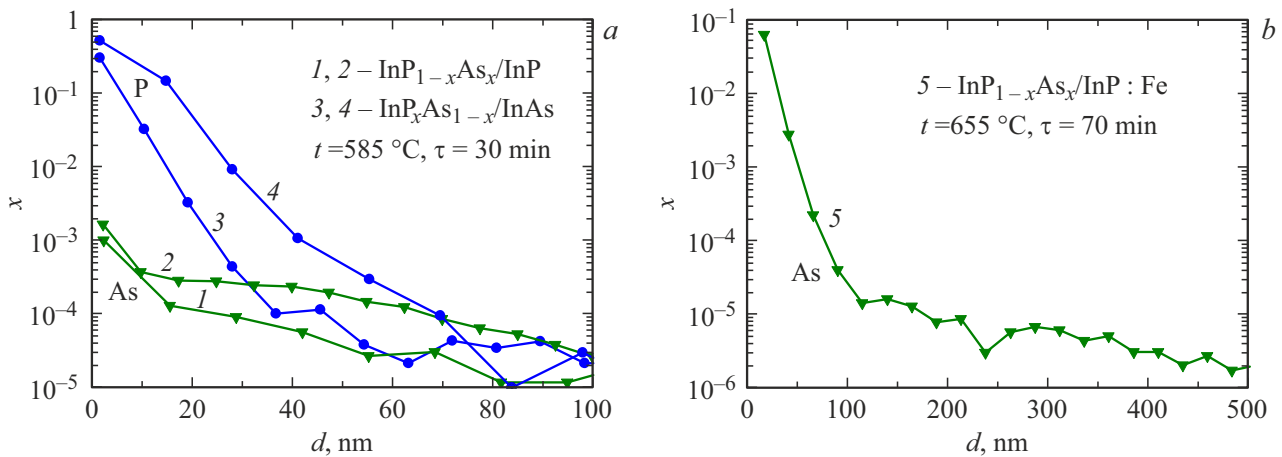
In the present study, we investigated solid-phase substitution of phosphorus with arsenic in InP(001) wafers and arsenic with phosphorus in InAs(001). The table

details the differences in conditions of synthesis of the examined samples:  $A^{III}B^V$  material type and volume density  $n$  of free electrons in the initial wafers, as well as individual process conditions. Prior to the solid-phase substitution process, the surface of wafers was subjected to anodic oxidation; the resulting oxide was removed in  $H_2O:HF$  (7:1). Solid-phase substitution was carried out in a heated quartz reactor in a hydrogen atmosphere. The initial  $A^{III}B^V$  wafers were introduced into one of the chambers in a closed graphite holder. The other chambers contained solution-melts serving as sources of vapors of fifth-group elements  $C^V$  and dopant impurity  $D^{II}$ ; all the chambers in the holder were interconnected.

Figure 1, *a* presents the results of secondary ion mass spectrometry (SIMS) measurements for the samples obtained at  $\tau = 30$  min and  $t = 585$  °C. It can be seen that the amount of phosphorus incorporated into InAs wafers (curves 3, 4 in Fig. 1, *a*) under the chosen conditions is two orders of magnitude higher than the amount of arsenic incorporated into InP (curves 1, 2 in Fig. 1, *a*), which is quite explicable if we take into account the difference in phosphorus and arsenic vapor pressures in the corresponding technological processes. According to our estimate obtained in [3] based on reference data [4,5], the phosphorus vapor pressure is two orders of magnitude higher than the arsenic vapor pressure at  $t$  and  $x_C^L$  values close to those at which samples Nos. 1–4 were synthesized in the present study. Increasing temperature  $t$ , holding time  $\tau$ , and atomic fraction of arsenic in the liquid phase  $x_C^L$  (see the table) for sample No. 5 based on InP, we managed to increase arsenic amount  $x$  in the near-surface layer of the formed  $InP_{1-x}As_x$  solid solution by at least an order of magnitude (Fig. 1, *b*).

Parameters of technological processes of synthesis of samples based on initial  $A^{III}B^V$  wafers

Sample number	Initial wafer $A^{III}B^V$		Individual process conditions				
	Wafer material	$n, \text{cm}^{-3}$	Substitution elements	$t, ^\circ\text{C}$	$\tau, \text{min}$	Solution-melt	$x_C^I$
1 (SPR117)	InP:S	$\sim 10^{18}$	Cd+As	585	30	Sn–CdGeAs <sub>2</sub>	0.05
2 (SPR118)	InP:Te	$\sim 10^{18}$					
3 (SPR116)	InAs:Sn	$\sim 10^{18} - 10^{19}$	Cd+P	585	30	Sn–CdGeP <sub>2</sub>	0.08
4 (SPR119)	InAs:Sn	$\sim 10^{18} - 10^{19}$	Cd+Zn+P	585	30	Sn–CdGeP <sub>2</sub> Sn–Zn <sub>3</sub> P <sub>2</sub>	0.08 0.05
5 (SPR193)	InP:Fe		As	655	70	Sn–InAs	0.16


**Figure 1.** Profiles of distribution of substitution fifth-group elements over depth  $d$  for samples Nos. 1–4 (a) and No. 5 (b). The curve numbers correspond to the sample numbers in the table.

Samples Nos. 1 and 2 based on InP wafers were obtained within the same technological process and shared the chamber of the graphite holder; i.e.,  $t$ ,  $\tau$ , and  $P_C$  were the same for them. However, SIMS studies revealed differences in the distribution of arsenic (Fig. 1, a) and cadmium (Fig. 2, a). These differences may be attributed to the difference in properties of the initial InP wafers, which were doped with different donor impurities (see the table).

The difference in distribution of embedded phosphorus for samples Nos. 3 and 4 based on InAs wafers taken from the same batch (Fig. 1, a) is attributable to the difference in process conditions: only one solution-melt was used for sample No. 3, while sample No. 4 was prepared from two different solution-melts positioned in different chambers (see the table), one of which served as a source of Zn vapor. It can be seen from Fig. 2, b that the Cd distribution profiles for samples Nos. 3 and 4 are similar in nature at a distance of 20 nm from the surface, but Cd was not detected by SIMS in sample No. 4 at depths greater than 20 nm. Figure 2, c shows the depth

distribution profile of Zn for sample No. 4. It is evident that Zn penetrates down to a significant depth (up to  $1.2 \mu\text{m}$ ), which is typical of this chemical element. In terms of their thickness and band gap  $E_g$  (according to calculations based on [6], their  $E_g = 0.5 - 0.7 \text{ eV}$ ), the near-surface layers of  $\text{InP}_x\text{As}_{1-x}$  solid solutions obtained this way in InAs wafers are suitable candidate materials for a wide-bandgap optical window of a photodetector based on InAs, which has  $E_g = 0.354 \text{ eV}$ .

The obtained results revealed that a temperature of at least  $655^\circ\text{C}$ , an increased concentration of arsenic in the solution-melt serving as its source ( $x_{\text{As}}^I \sim 0.16$ ), and a long holding time (close to an hour) are required for the formation of near-surface regions of  $\text{InP}_{1-x}\text{As}_x$  solid solutions in InP wafers with  $x \sim 0.1$  at depths  $d = 20 - 40 \text{ nm}$ . Near-surface layers of  $\text{InP}_x\text{As}_{1-x}$  solid solutions with  $x$  up to  $0.2 - 0.4$  may be formed at depths up to 20 nm in InAs wafers at lower temperatures (approximately  $585^\circ\text{C}$ ), half the holding time, and with a lower phosphorus concentration in the solution-melt ( $x_{\text{P}}^I = 0.05 - 0.07$ ).

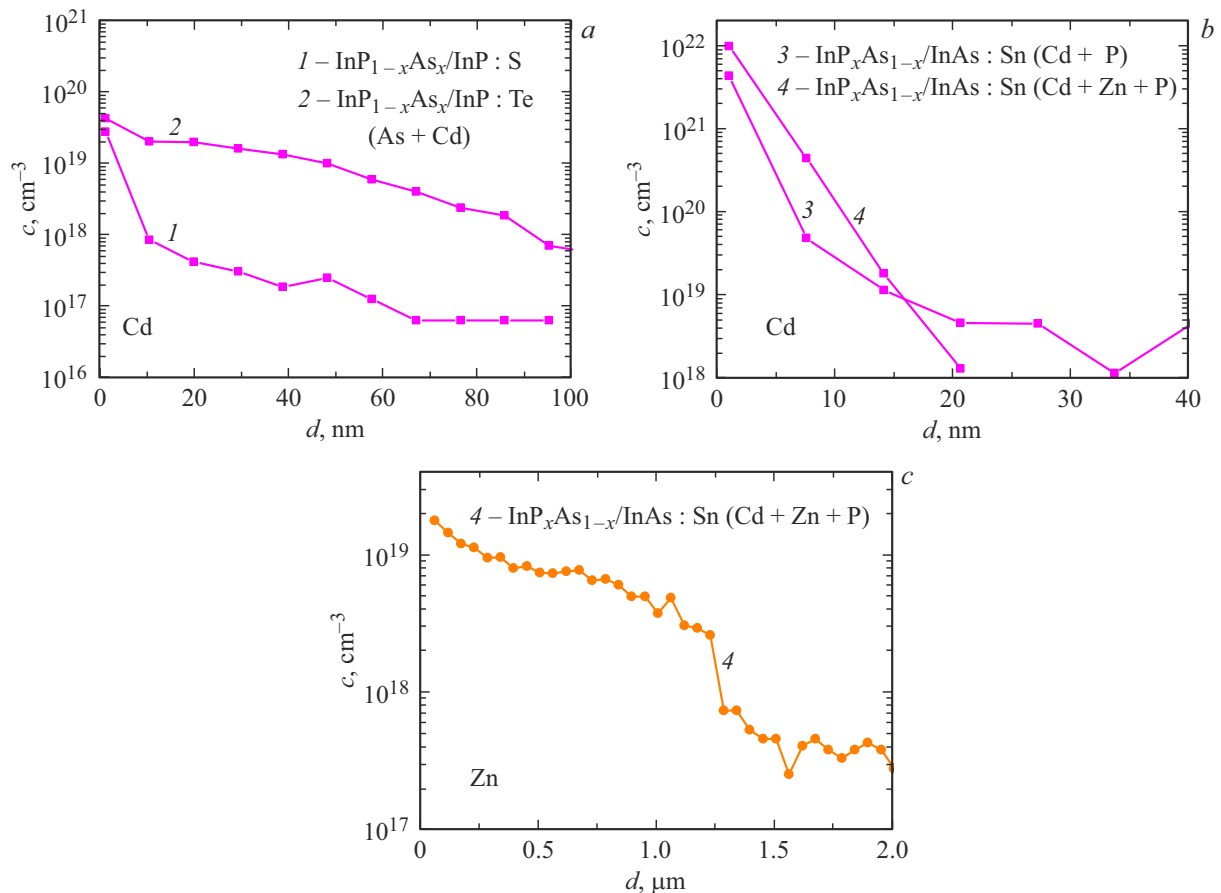


**Figure 2.** Dependences of volume density  $c$  of dopant impurities on depth  $d$  for Cd in samples Nos. 1, 2 based on InP of different doping types (a), for Cd in samples Nos. 3, 4 based on InAs:Sn (b), and for Zn in sample No. 4 based on InAs:Sn (c). The curve numbers correspond to the sample numbers in the table.

## Acknowledgments

The authors wish to thank Yu.K. Undalov for providing the materials for  $\text{D}^{\text{II}}\text{E}^{\text{IV}}\text{C}_2^{\text{V}}$  ternary compounds.

## Funding

Equipment provided by Common Use Center „Materials Science and Diagnostics in Advanced Technologies“ (Ioffe Institute), which is supported by the Ministry of Science and Higher Education of Russia, was used for SIMS studies.

## Conflict of interest

The authors declare that they have no conflict of interest.

## References

- [1] V.P. Khvostikov, S.V. Sorokina, O.A. Khvostikova, M.V. Nakhimovich, M.Z. Shvarts, *Semiconductors*, **55**, 840 (2021). DOI: 10.1134/S1063782621100134.
- [2] V.I. Vasil'ev, G.S. Gegis, V.I. Kuchinskii, V.G. Danil'chenko, *Semiconductors*, **49**, 962 (2015). DOI: 10.1134/S1063782615070234.

- [3] G.S. Gegis, V.I. Kuchinskii, D.Yu. Kazantsev, B.Ya. Ber, M.V. Tokarev, V.P. Khvostikov, M.V. Nakhimovich, A.S. Vlasov, V.I. Vasil'ev, *Tech. Phys. Lett.*, **48** (11), 1 (2022). DOI: 10.21883/TPL.2022.11.54876.19304.
- [4] A. Smits, S.C. Bokhorst, *Z. Phys. Chem.*, **91U** (1), 249 (1916). DOI: 10.1515/zpch-1916-9114
- [5] B.E. Poling, G.H. Thomson, D.G. Friend, R.L. Rowley, W.V. Wilding, in *Perry's chemical engineers' handbook*, ed. by D.W. Green, R.H. Perry, 8th ed. (The McGraw-Hill Companies, Inc., N.Y., 2008), section 2.
- [6] I. Vurgaftman, J.R. Meyer, L.R. Ram-Mohan, *J. Appl. Phys.*, **89** (11), 5815 (2001). DOI: 10.1063/1.1368156

Translated by D.Safin